Electromagnetic Calculation and Plasma Leakage Rate Analysis of the Magnetically Confined Plasma Rocket

2008 Plasma Sci. Technol. 10 211

(http://iopscience.iop.org/1009-0630/10/2/15)

Electromagnetic Calculation and Plasma Leakage Rate Analysis of the Magnetically Confined Plasma Rocket*

NI Zhipeng (倪志鹏)[1], WANG Liangbin (汪良斌)[1], CHEN Zhiyou (陈治友)[2], ZHANG Yong (张勇)[2], WANG Futang (王福堂)[2], LI Jiangang (李建刚)[1]

[1]Institute of Plasma Physics, Chinese Academy of Sciences, Hefei 230031, China
[2]Hefei High Magnetic Field Laboratory, Chinese Academy of Sciences, Hefei 230031, China

Abstract An electromagnetic calculation and the parameters of the magnet system of the magnetically confined plasma rocket were established. By using ANSYS code, it was found that the leakage rate depends on the current intensity of the magnet and the change of the magnet position.

Keywords: magnetically confined plasma rocket, plasma leakage rate, electromagnetic calculation

PACS: *52.75.Di, 52.55.Jd, 47.11.Fg*

1 Introduction

Plasma, known as the fourth state of matter, is an ionized gas constituted by atoms stripped of electrons. The plasma is also a good electrical conductor. The plasma can be captured, moved and accelerated with an ingeniously designed magnetic field.

The concept of magnetically confined plasma rocket based on magnetic mirror fundamental [1], makes use of a semi-open magnetic mirror configuration to control and confine the plasma. The magnetically confined plasma rocket contains three connective magnetic mirror cells: front, middle, and rear. During the rocket operation, neutral gas (typically hydrogen) is injected into the front cell and ionized. The resultant plasma is heated through radio frequency (RF) wave-plasma interaction, e.g., ion cyclotron resonance heating in the middle cell to the desired temperature and density. After heating, the plasma is magnetically (and gasdynamically) exhausted at the rear cell to provide modulated thrust [2,3]. The magnetically confined plasma rocket has been under development by scientists in the United State since the 1980s. A 10-kilowatt magnetic confinement plasma rocket [4] was set up. The advantage of the magnetically confined plasma rocket is that it has a high specific impulse and can change and adjust the plasma state to keep up the best propulsion efficiency. This rocket can be used to increase the traveling speed in interplanetary space, and shorten the traveling time compared with a traditional rocket [5,6]. In the rocket, the specific impulse is usually determined as the exhaust velocity divided by the acceleration of gravity at sea level (9.8 m/s^2). With a given payload, the higher the specific impulse of the rocket is, the faster the rocket flies. The magnetically confined plasma rocket derives the thrust from high temperature plasmas [7]. As is known, the temperature of the plasma can reach a few million Celsius degrees. At a high temperature, ions move at a velocity of about 3×10^5 m/s [4]. Hence, the specific impulse is very high, about 3×10^4 seconds. However, the traditional rocket depends on the gas created from the combustion of chemical fuel. The gas is exhausted backward at high speed while the rocket achieves the thrust in the front direction [8]. Because the temperature of the exhausted gas is only about a few thousand Celsius degrees [4], its impulse is very low compared to that of the magnetically confined plasma rocket. If a traditional rocket travels between the Earth and the Mars with the same payload, it will take about ten months to fly from the Earth to the Mars, but a magnetically confined plasma rocket will only take about four months [4], since its specific impulse is much larger than that of the traditional rocket. In addition the magnetically confined plasma rocket can reduce the radiation effect on the human immune system and the weakness of bone and muscle due to a short travel time. To our knowledge, there has been little research about the magnetically confined plasma rocket in China. We are working on setting up a magnetically confined plasma rocket system for future interplanetary travel and space science research.

2 Structure of the magnet system and the electromagnetic calculation

2.1 Structure of the magnet system and design requirements

The magnet system of the magnetically confined plasma rocket is composed of four solenoid supercon-

*supported by the Fund of Knowledge Innovation Program of Chinese Academy of Sciences (No. KJCX2-SW-N19)

ducting magnets. They have a common axis and are laid in an order shown in Fig. 1. All the four magnets have an inner diameter of 197.78 mm and a length of 100 mm. The magnets are set apart at a distance of 270 mm, 370 mm, 270 mm, respectively. The central magnetic induction of magnet-1 and magnet-2 is required to reach 0.5 Tesla while the central magnetic induction of magnet-3 and magnet-4 is to reach 1.0 Tesla. In our case Magnet-4 acts as the nozzle of the magnet system. The distance among the four magnets is defined according to the design requirements of the size of the Dewar containers, and heating and detection equipment. The diameter of the Russia made NbTi superconducting wires is 0.87 mm with a ratio of copper to superconductor of 1.38 : 1. The critical current of the superconducting wires is 550 A at a temperature of 4.2 K and a magnetic field of 5.0 T. These wires can meet the requirement for the coils to produce a magnetic field of 1.0 T.

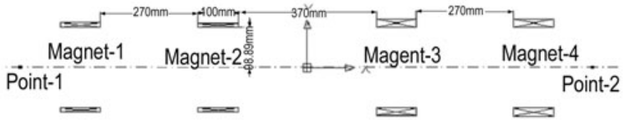

Fig.1 Layout of the magnet system

2.2 Electromagnetic calculation

According to the ANSYS code, we need to set up a model of the magnet system. Because the magnetic coil is axisymmetric, so a two dimension model is adopted for the electromagnetic calculation. With this model, three regions can be defined, the far-field region, the near-field region and the magnet region, as shown in Fig. 2. Supposing that there is no magnetic induction far from the magnet system, e.g., beyond 10 m as is set in our calculation. We define the region between 5 m and 10 m as the far-field region which means the region between the large half circle and the small half circle, the region between the outside of the magnets and 5 m as the near-field region which is the small half circle region except the four magnets, and the magnet region which is the four magnets made into four rectangles, respectively. In order to show the four magnets clearly, a magnified figure is given in Fig. 3. Based on the model, we divide the meshes in the three regions as shown in Fig. 4 and Fig. 5. In the far-field region, the magnetic induction is weak, and the density of meshes is low, as shown in Fig. 4. In the near-field region and magnet region, the magnetic induction is stronger than that in the far-field, so more meshes are set. The magnified meshes in the region around magnet-2 and magnet-3 are shown in Fig. 5. The calculated results of the distribution of the magnetic flux, magnetic induction and central magnetic induction are shown in Fig. 6, Fig. 7 and Fig. 8, respectively.

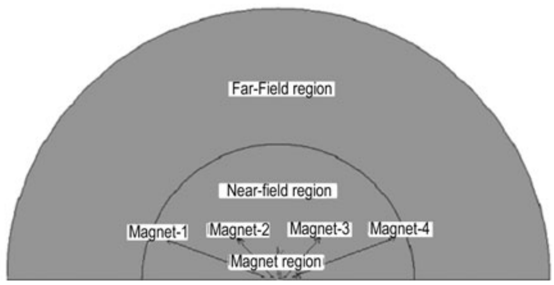

Fig.2 Model of electromagnetic calculation

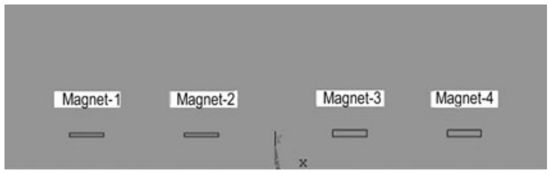

Fig.3 Magnification of four magnet models

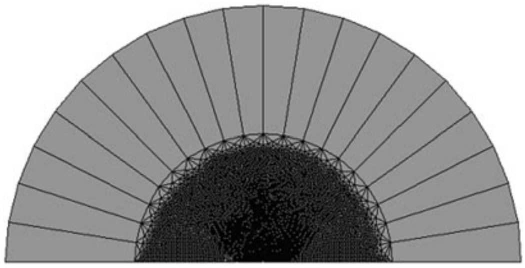

Fig.4 Mesh division of the magnet system model

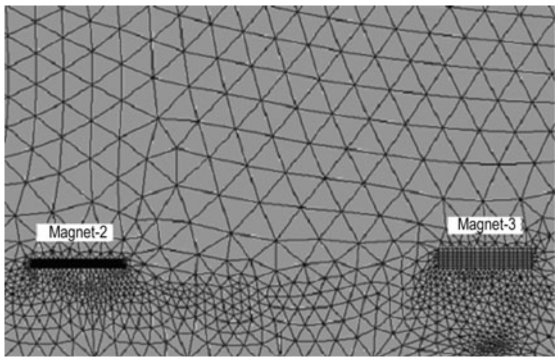

Fig.5 Magnification of meshes around magnet-2 and magnet-3

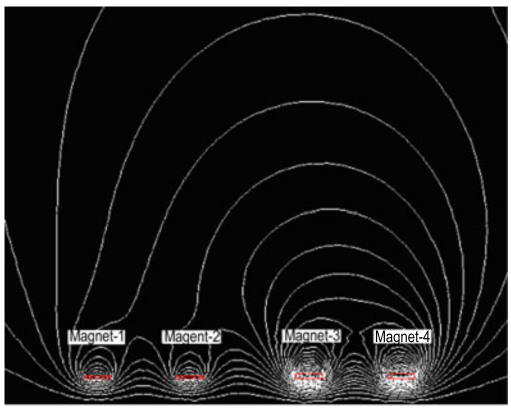

Fig.6 Distribution of the magnetic flux

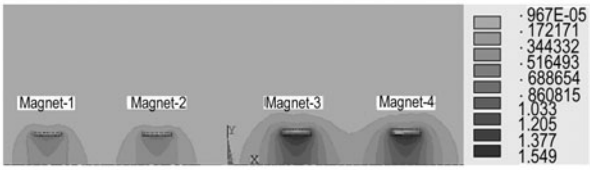

Fig.7 Nephogram of the magnetic induction

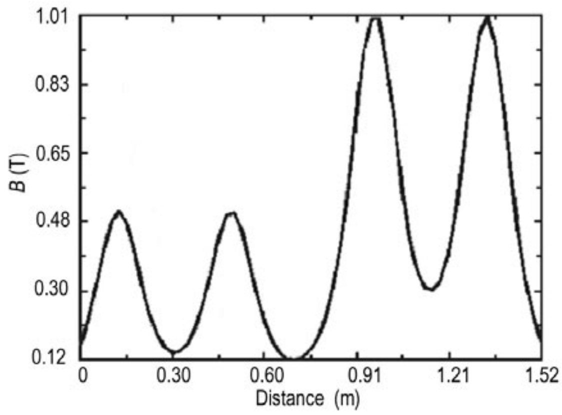

Fig.8 Magnetic induction distribution along the axis

Fig. 8 is the magnetic induction distribution of the magnet system at the central axis between point-1 and point-2. There are four peak values in the distribution of magnetic induction, which are the central magnetic induction of the magnet-1, magnet-2, magnet-3 and magnet-4 from left to right. According to the result of the magnetic induction calculation, the specific magnet parameters can be derived and listed in Table 1.

3 Plasma leakage rate analysis of the magnet system of the magnetically confined plasma rocket

3.1 Plasma leakage rate of the magnet system

In the magnetically confined plasma rocket, the four magnets form three magnetic mirrors, and the thrust of the rocket is generated by the escaping high energy particles in the magnetic mirror, as mentioned above. The plasma leakage rate of the magnetic mirror can be evaluated by the escape probability of the particles in the magnetic mirror. The structure of the magnetic mirror consists of two magnetic coils having the same current direction and an axisymmetric longitudinal filed, as shown in Fig. 9 [9]. The magnetic field is the strongest at the centre of the two magnetic coils, and weakest at the middle point between them. According to the theory of the magnetic mirror plasma, if we neglect Coulomb collisions of charged particles and effects caused by magneto-hydrodynamic instabilities, then the magnetic moment and total kinetic energy of the charged particles are conserved [10]. The transverse velocity of the charged particle is greater at the high magnetic field region while the total kinetic energy of the charged particles keeps the same so that the longitudinal velocity is lower, and the charged particles are reflected back and confined. The transverse velocity is lower while the longitudinal velocity is greater at the weak magnetic field region. If the charged particles still keep a high longitudinal velocity through the strongest magnetic field, they will escape through the magnetic coils.

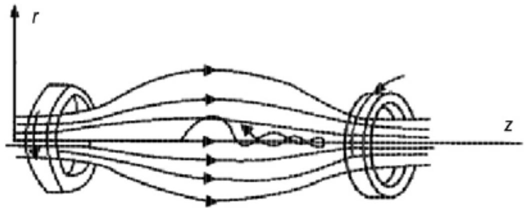

Fig.9 Principle drawing of the magnetic mirror

Some charged particles can be confined, and become the trapped particles for the specified magnetic mirror field, but others can escape through the magnetic coil. The escaping probability of charged particles depends on a critical angle related to the magnetic induction [11].

$$\sin^2\theta_c = \frac{B_0}{B_m}, \tag{1}$$

Here, B_0 is the weakest magnetic induction in the magnetic mirror, B_m is the strongest at the centre of the magnetic coil, θ_c is the critical angle of the escaping charged particles. As the angle between the velocity direction of the charged particles and B_0 is larger than θ_c, the charged particles will be trapped in the magnetic mirror region. However, when the angle is less than θ_c, the charged particles will escape through the magnetic mirror region. Then a escaping cone in the velocity distribution functions of the plasma is formed with a width of $2\theta_c$ in velocity space. The charged particles in the cone will escape from the magnetic mirror, and the charged particles out of the cone will be trapped. Suppose that the velocity distribution of the plasma is isotropic, the escaping probability of the charged particles, i.e., the plasma leakage rate, can be expressed as [12].

$$\begin{aligned} P_{\text{leakage rate}} &= \frac{1}{2\pi}\int_0^{\theta_c} 2\pi \sin\theta \mathrm{d}\theta = 1 - \cos\theta_c \\ &= 1 - \sqrt{1 - \frac{B_0}{B_m}}, \end{aligned} \tag{2}$$

Here, $P_{\text{leakage rate}}$ is the escaping probability of charged particles. From the ANSYS calculation, we found that for magnet-3 and magnet-4 B_m is 1.00 Tesla, and B_0 is 0.30 Tesla. Putting B_m and B_0 into Eq. (1) and (2), we find that θ_c is about 33.21° and the leakage rate $P_{\text{leakage rate}}$ is 0.1633. This means that 16.33% charged particles will escape from the magnetic mirror under the condition of the required magnet structure as shown in Table 1.

Table 1. Magnets parameters

Parameter	Magnet-1	Magnet-2	Magnet-3	Magnet-4
Inner diameter(mm)	197.78	197.78	197.78	197.78
Outer diameter (mm)	215.66	215.22	235	235.18
Magnets length (mm)	100	100	100	100
Central magnetic induction (T)	0.50	0.50	1.00	1.00
Current density (A/m^2)	9.88×10^7	9.88×10^7	9.88×10^7	9.88×10^7
Total turn	1104	1077	2299	2310

3.2 Influence of the position and current of the magnets on the leakage rate

$P_{\text{leakage rate}}$ can be adjusted by changing the magnets' positions and coil currents.

First, we change the axial position of magnet-4 in the magnetic mirrors, and fix the current of the four magnets. The calculated data of the leakage rate are shown in Fig. 10. In Fig. 10, $R_4^{'} - R_4^0$ is the relative axial position of magnet-4. The original position of magnet-4 is shown in Fig. 1. The negative value of $R_4^{'} - R_4^0$ means that magnet-4 moves toward magnet-3 while a positive value of $R_4^{'} - R_4^0$ means that magnet-4 moves away from magnet-3.

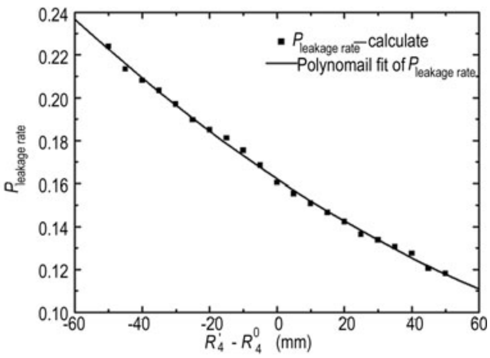

Fig.10 Relationship of the leakage rate $P_{\text{leakage rate}}$ and the relative position $R_4^{'} - R_4^0$ between magnet-3 and magnet-4

We can fit the data in Fig. 10 with a formular of $P_{\text{leakage rate}} = 0.16 - 0.0011 \times (R_4^{'} - R_4^0) + 3.21 \times 10^{-6} \times (R_4^{'} - R_4^0)^2$ with $R_4^{'} - R_4^0$ in millimeter. It is seen that the relationship of the leakage rate and the relative position of magnet-4 is linear basically. With the shortening of the distance between magnet-3 and magnet-4, the leakage rate will increase monotonically. That is because the value of B_0/B_{m} will increase with the shortening of the distance. Therefore, $P_{\text{leakage rate}}$ will tend to increase monotonically. When the distance between magnet-3 and magnet-4 increases, $P_{\text{leakage rate}}$ decreases monotonically.

Fixing the position of the magnets and the currents of magnet-1, magnet-2, and magnet-3 in Fig. 1, and changing the current of magnet-4, we can investigate the influence of the magnetic induction of magnet-4 on the $P_{\text{leakage rate}}$. The resultant data are shown in Fig. 11.

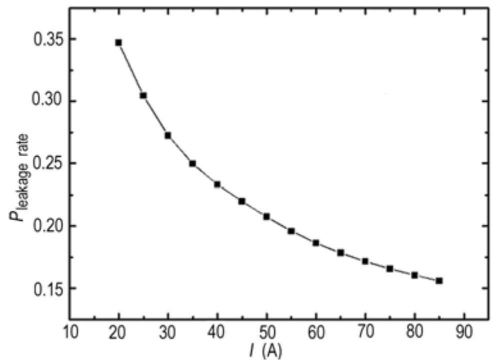

Fig.11 Relationship of the leakage rate $P_{\text{leakage rate}}$ and the current I of magnet-4

It is shown that when the current in magnet-4 increases, the leakage rate will be reduced, which is because the value of B_0/B_{m} becomes smaller when the current of magnet-4 increased. However, when the current of magnet-4 decreases, the leakage rate increases, which is because the value of B_0/B_{m} becomes greater when the current of magnet-4 decreases.

4 Conclusion

We calculated the specific magnet parameters of the magnetically confined plasma rocket by ANSYS code. It was found that the plasma leakage rate of the rocket increases with both the decrease in the distance between magnet-3 and magnet-4, and the decrease in the current of magnet-4. These calculation results may provide some useful ideas for future physical experiments.

References

1 Zhu Shiyao. 1992, Fundamentals of Nuclear Fusion. Hefei: University of Science and Technology of China Press. p.66 (in Chinese)

2 Alexey V A, Breizman B N. 2005, Physics of Plasmas, 12: 043504

3 Ilin A V, Chang Diaz F R, Squire J P, et al. 2004, Simulations of Plasma Detachment in VASIMR. 42nd American Institute of Aeronautics and Astronautics (AIAA), Aerospace Sciences Meeting and Exhibit., Reno, Nevada, 5-8 January 2004. AIAA-2004-0151

4 Chang Diaz F R. 2000, Scientific American, 283: 9

5 Chang Diaz F R, Braden E, Johnson I, et al. 1995, Rapid Mars Transits with exhaust-modulated plasma propulsion. Houston: NASA Johnson Space Center. NASA Technical Paper 3539

6 Yang Liming, CAO Xiangyu. 2002, Aerospace Shanghai, 2: 53 (in Chinese)
7 Breizman B N, Arefier A V. 2001, Physics of Plasmas, 8: 907
8 Lu Xin, Zhang Jie, Li Yingjun. 2002, Physics & High and New Technology, 31: 796 (in Chinese)
9 Yao Ruohe, Wu Weijing, Zhang Xiaodong, et al. 2004, Vacuum Science and Technology, 24: 105 (in Chinese)
10 Golant V E, Zhilinsky A P, Sakharov I E. 1980, Fundamentals of Plasma Physics. New York: John Wiley & Sons, Inc. p.262
11 Chen Francis F. 1981, Introduction to Plasma Physics. translated by G.H.Lin. Beijing: People's Education Press. p.18 (in Chinese)
12 Xu Jialuan, Jin Shangxian. 1981, Plasma Physics. Beijing: Atomic Energy Press. p.91 (in Chinese)

(Manuscript received 16 March 2007)

E-mail address of WANG Liangbin: wanglb@ipp.ac.cn